Biochimica et Biophysica Acta 1842 (2014) 2246–2256

Contents lists available at ScienceDirect

Biochimica et Biophysica Acta

journal homepage: www.elsevier.com/locate/bbadis

Novel role of silent information regulator 1 in acute endothelial cell oxidative stress injury

Yue Li [a,1], Kun Wang [b,1], Yingtong Feng [c,d,1], Chongxi Fan [c], Feng Wang [e], Juanjuan Yan [a], Jian Yang [f], Haifeng Pei [f], Zhenxing Liang [f], Shuai Jiang [a], Xiangjun Chen [g], Yang Yang [a,h,*], Yan Qu [a,*]

[a] Department of Neurosurgery, Xijing Hospital, The Fourth Military Medical University, 127 Changle West Road, Xi'an 710032, China
[b] Department of Medical Management, Chinese PLA General Hospital, Beijing 100048, China
[c] Department of Thoracic Surgery, Tangdu Hospital, The Fourth Military Medical University, 1 Xinsi Road, Xi'an 710038, China
[d] Department of Cardiothoracic Surgery, The 97th Hospital of PLA, 226 Tongshan Road, Xuzhou 221004, China
[e] Department of Anesthesiology, Xijing Hospital, The Fourth Military Medical University, 127 Changle West Road, Xi'an 710032, China
[f] Department of Cardiovascular Surgery, Xijing Hospital, The Fourth Military Medical University, 127 Changle West Road, Xi'an 710032, China
[g] Department of Stomatology, The 253rd Hospital of PLA, 111 Aimin Road, Hohhot 010051, China
[h] Department of Medical Administration, Beidaihe Sanatorium, Beijing Military Area Command, 4 West Beach Road, Qinhuangdao 066100, China

ARTICLE INFO

Article history:
Received 28 March 2014
Received in revised form 5 August 2014
Accepted 7 August 2014
Available online 14 August 2014

Keywords:
Silent information regulator 1
Acute oxidative stress injury
EX527
Mitogen activated protein kinases

ABSTRACT

Silent information regulator 1 (SIRT1), a class III histone deacetylase, retards aging and plays roles in cellular oxidative stress injury (OSI). However, the biological context in which SIRT1 promotes oxidative injury is not fully understood. Here, we show that SIRT1 essentially mediates hydrogen peroxide (H_2O_2)-induced cytotoxicity in human umbilical vein endothelial cell (HUVEC). In HUVECs, SIRT1 protein expression was significantly increased in a dose-dependent manner after H_2O_2 treatment, whereas the acetylation levels of the NF-κB p65 subunit and p53 were decreased. EX527 (a specific SIRT1 inhibitor) conferred protection to the HUVECs against H_2O_2, as indicated by an improved cell viability, adhesion, an enhanced migratory ability, a decreased apoptotic index, decreased reactive oxygen species (ROS) production and reductions in several biochemical parameters. Immunofluorescence and Western blot analyses demonstrated that H_2O_2 treatment up-regulated SIRT1, phosphorylated-JNK (p-JNK), p-p38MAPK, and p-ERK expression. EX527 pretreatment reversed these effects on SIRT1, p-JNK, and p-p38MAPK but further increased the p-ERK levels. Similar results were confirmed in SIRT1 siRNA experiments. In summary, SIRT1 signaling pathway inhibition imparts protection against acute endothelial OSI, and modulation of MAPKs (JNK, p38MAPK, and ERK) may be involved in the protective effect of SIRT1 inhibition.

1. Introduction

The endothelium plays a critical role in the regulation of vascular function and the development of physiological and pathophysiological processes [1]. Endothelial dysfunction has been observed in patients with atherosclerosis, hyperlipidemia, diabetes, hypertension, aging, and obesity [2,3]. Oxidative stress injury (OSI) plays an essential role in the pathogenesis of cardiovascular and non-cardiovascular diseases, including endothelial dysfunction [3,4]. Multiple cytokines and signaling pathways have been implicated in oxidative stress-mediated vascular damage [5,6]. However, the underlying pathophysiological mechanisms of OSI have not been fully elucidated.

Silent information regulator 1 (SIRT1) is a nicotinamide adenine dinucleotide (NAD^+)-dependent histone deacetylase. Among the seven human sirtuins, SIRT1 is the most extensively studied [7]. Many studies have found that SIRT1 plays an important role in extending life-span and calorie restriction [8]. Nevertheless, SIRT1 activation is not always beneficial for fighting diseases [9,10]. Additionally, it is not clear whether SIRT1 is inhibited or activated by OSI [11–16]. On the one hand, studies have suggested that SIRT1 is down-regulated in OSI and that SIRT1 up-regulation may be beneficial for OSI [12–14]. On the other hand, other studies have demonstrated that SIRT1 is up-regulated in OSI [15,16]. In this study, we explore the role of SIRT1 in hydrogen peroxide (H_2O_2)-induced acute endothelial cell OSI.

Abbreviations: SIRT1, silent information regulator 1; OSI, oxidative stress injury; HUVECs, human umbilical vein endothelial cells; H_2O_2, hydrogen peroxide; ROS, reactive oxygen species; NAD^+, nicotinamide adenine dinucleotide; JNK, c-Jun N-terminal kinase; p38MAPK, p38mitogenactivated protein kinase; ERK, extracellular signal regulated kinase; p-p38MAPK, phosphorylated-p38MAPK; DAPI, 4′,6-diamino-2-phenylindole; DMSO, dimethylsulfoxide; DCFH-DA, 2′,7′-dichlorofluorescein diacetate; TUNEL, Terminal deoxynucleotidyl transferase dUTP nick end-labeling; LDH, lactate dehydrogenase; MDA, methane dicarboxylic aldehyde; SOD, superoxide dehydrogenase; GSH-Px, glutathione peroxidase; CCK8, Counting Kit-8; OD, optical density; TBST, Tris-buffered saline and Tween 20; SD, standard deviation; ox-LDL, oxidized low-density lipoprotein; COPD, chronic obstructive pulmonary disease; Akt, protein kinase B; ASK1, apoptosis signal-regulating kinase 1

* Corresponding authors at: Department of Neurosurgery, Xijing Hospital, 127 Changle West Road, Xi'an 710032, China. Tel.: +86 29 84775324; fax: +86 29 84775567.
E-mail addresses: yang200214yy@163.com (Y. Yang), yanqu1974@126.com (Y. Qu).
[1] These authors contributed equally to this work.

http://dx.doi.org/10.1016/j.bbadis.2014.08.003
0925-4439/

Endothelial cell apoptosis and death are induced during OSI by activating injury-related kinases, including c-Jun N-terminal kinase (JNK), p38mitogenactivated protein kinase (p38MAPK), and extracellular signal regulated kinase (ERK), which are induced by physical, chemical, and physiological stressors [17,18]. The transient activation of these kinases in response to OSI cytokines promotes endothelial cell proliferation and survival, whereas the prolonged activation of these kinases may result in endothelial cell death through the modulation of pro- and anti-apoptotic protein functions [19–21]. In this study, we also explore the effects of SIRT1 on these kinases in endothelial cell OSI.

2. Materials and methods

2.1. Materials

EX527 (a specific SIRT1 inhibitor) was purchased from Tocris Bioscience (Bristol, UK); SIRT1 siRNA and anti-phosphorylated-p38MAPK (p-p38MAPK), p38MAPK, p-JNK, JNK, and SIRT1 antibodies were obtained from Santa Cruz Biotechnology (Santa Cruz, CA, USA). Anti-p-ERK, ERK, acetylated-p53 (Ac-p53), Ac-NF-κBp65, and β-actin antibodies were purchased from Cell Signaling Technology (Beverly, MA, USA). Anti-superoxide dehydrogenase (Cu/Zn-SOD or SOD) and glutathione peroxidase (GSH-Px) antibodies were purchased from Abcam Company (Cambridge, UK). 4′,6-Diamino-2-phenylindole (DAPI), 3-(4,5-dimethylthiazol-2-yl)-2, 5-diphenyltetrazolium bromide (MTT), dimethylsulfoxide (DMSO), and 2′,7′-dichlorofluorescein diacetate (DCFH-DA) were purchased from Sigma-Aldrich (St. Louis, MO, USA). Terminal deoxynucleotidyl transferase dUTP nick end-labeling (TUNEL) kits were purchased from Roche (Mannheim, Germany). The Cell Counting Kit-8 (CCK8) was purchased from Dojindo (Kumamoto, Japan). Kits for lactate dehydrogenase (LDH), methane dicarboxylic aldehyde (MDA), SOD, and GSH-Px concentration measurements were purchased from the Institute of Jiancheng Bioengineering (Nanjing, Jiangsu, China). Rabbit anti-goat, goat anti-rabbit, and goat anti-mouse secondary antibodies conjugated with horseradish peroxidase or tetraethyl rhodamine isothiocyanate (TRITC) were purchased from Zhongshan Company (Beijing, China).

2.2. Cell culture and treatments

HUVECs (ATCC CRL-1730; Shanghai Tiancheng Technology Company, China) were cultured in DMEM medium (Hyclone, UT, USA) supplemented with fetal calf serum (10%), 2 mM L-glutamine, 100 U/ml penicillin, and 100 g/ml streptomycin at 37 °C in 5% CO_2 and 95% air. The EX527 stock solution was prepared in DMSO and diluted with culture medium immediately prior to use; 0.01% DMSO was used as a sham control. The cells were pre-treated with EX527 (12 h) or SIRT1 siRNA for 24 h and were then subjected to H_2O_2 (100, 200, 300, or 400 μM) injury (4 h). H_2O_2 concentrations and durations were selected based on our previous studies [3]. Cells were harvested after treatment for further analysis.

2.3. Cell viability analysis

Cell viability was detected using the CCK8 assay following the manufacturer's instructions. Briefly, after the cells were treated and washed with PBS, 10 μl CCK8 and 100 μl DMEM were added to each well. After 2 h incubation, absorbance was measured using a microtiter plate reader (SpectraMax 190, Molecular Device, CA, USA) at 450 nm. Cell viability was expressed as an optical density (OD) value. Cell morphologies were observed, and images were obtained using an inverted/phase contrast microscopy (Olympus BX61, Japan).

2.4. SIRT1 activity analysis

SIRT1 activity analysis was performed as previously described [22]. After being treated, HUVECs were homogenized in an ice-cold lysis buffer (50 mM Tris–HCl (pH 7.4), 150 mM of NaCl, 1 mM of phenylmethylsulfonyl fluoride (FMSF), 5 μg/ml of aprotinin), and proteins in the supernatant were extracted following centrifugation (15,000 rpm, 10 min, 4 °C). The SIRT1 activity in the total protein samples was determined using a histone deacetylase (HDAC) colorimetric assay kit (Enzo life Science, New York, NY, USA) according to the manufacturer's instructions.

2.5. LDH release analysis

LDH is of medical significance because it is found extensively in body tissues and cells, including vascular endothelial cells. Because it is released during cell damage, it is a common marker of injuries and diseases [23]. LDH was detected after H_2O_2 exposure using an assay kit according to the manufacturer's protocol. Enzyme activity was expressed as units per liter, and the absorbance was measured at 440 nm.

2.6. Intracellular MDA, SOD, and GSH-Px content analysis

MDA, SOD, and GSH-Px activities were all determined using commercially available kits, and all of the procedures complied with their respective manufacturer's instructions. Enzyme activities were expressed as units per milligram of protein. MDA is an organic compound with a molecular formula of $CH_2(CHO)_2$. MDA is generated from reactive oxygen species (ROS) and, as such, is assayed as a bio-marker of oxidative stress [24]. MDA content was measured at 532 nm by reaction with thiobarbituric acid to form a stable chromophore. The MDA levels were expressed as nanomoles per milligram of protein. The endothelial cells are able to express several antioxidants, such as SOD and GSH-Px, along with other enzymatic and non-enzymatic antioxidants to prevent free-radical damage and ROS-induced cellular damage [3,5]. The SOD activity assay was based on its ability to inhibit hydroxylamine oxidation by the O^{2-} produced via the xanthine–xanthine oxidase system. One unit of SOD activity was defined as the amount that reduced the absorbance by 50% at 550 nm. GSH-Px activity was determined by quantifying the ratio of reduced GSH to oxidized GSH after oxidation by H_2O_2. One unit of GSH-Px was defined as the amount that reduced 1 μM GSH in 1 min/mg protein at 412 nm.

2.7. Intracellular ROS content analysis

The intracellular ROS was measured using 2′,7′-DCFH-DA reagent. DCFH-DA enters through the cell membrane and is enzymatically hydrolyzed by intracellular esterases to non-fluorescent DCFH-DA, which is then oxidized to highly fluorescent DCFH in the presence of intracellular ROS [25]. Briefly, after cells were seeded and treated in opaque 96-well plates, the cells were washed with PBS (pH 7.4) and incubated with DCFH-DA (20 μM) in PBS at 37 °C for 2 h. After incubation, the cellular DCFH fluorescence in each well was measured at 530 nm emission and 485 nm excitation using an FLX 800 microplate fluorescence reader (Biotech Instruments, Inc., USA). Cell-free conditions were used as the background. The results were expressed as the percentage of the control group (100%) fluorescence intensity.

2.8. Cellular apoptosis analysis

Cellular apoptosis was analyzed by performing a TUNEL assay using an in situ cell death detection kit. A double-staining technique was used according to the manufacturer's instructions. After the cells were fixed in paraformaldehyde (4%, w/v) for 24 h, the TUNEL assay was performed to stain apoptotic cell nuclei (green), and DAPI was used to

stain all nuclei (blue). The apoptotic index was expressed as the ratio of positively stained apoptotic cells to the total number of cells counted × 100%.

2.9. Cellular adhesion ability assay

The procedure was performed according to a previously described method [20] with minor modifications. Briefly, after centrifugation and resuspension in basal medium with 5% fetal bovine serum, treated HUVECs (1×10^4 cells per well) were placed on fibronectin-coated 96-well plates and incubated for 30 min at 37 °C. Gentle washing was performed 3 times with PBS after 30 min adhesion. Adherent cells were stained with MTT and counted by independent blinded investigators. The number of adherent cells in the control group was set to 100%.

2.10. Wound healing assay

Cells were seeded in 6-well plates and treated for different periods. As previously described [5], confluent cell monolayers were scratched with a P200 pipette tip to produce three parallel "wounds" in each well; then, the cells were incubated with 5% fetal bovine serum for 24 h. Migrated cells were photographed and images were obtained using an inverted/phase-contrast microscopy (Olympus BX61, Japan). Due to the injury, endothelial cell growth and proliferation decreased; in fact, monolayers with scratch wounds were observed to slowly "heal" or, in some cases, not even recover compared with protected cells. The mean distance between the two ends of each scratch wound was quantified manually. The control was set to 100%.

2.11. Immunofluorescence assay

After cells were fixed in paraformaldehyde (4%) for 24 h, they were permeabilized in 0.1% Triton X-100 for 10 min and blocked in 5% bovine serum albumin for 30 min at room temperature. Cells were then incubated with anti-SIRT1 rabbit polyclonal antibodies (1:200) overnight at 4 °C. Following PBS washes, the cells were incubated with TRITC-conjugated goat anti-rabbit secondary antibodies (1:200) for 2 h. The cells were subsequently incubated with DAPI (0.02 mg/ml) for 2 min, washed with PBS and wet-mounted using glycerol (50%, v/v). Images were taken under fluorescence microscopy (BX51, Olympus, Japan) with a CCD camera (DP70, Olympus, Japan).

2.12. Protein extract preparation and Western blotting

Cells were homogenized in lysis buffer (Beyotime Biotechnology, Haimeng, Jiangsu, China) with a 1% protease inhibitor cocktail (Sigma-Aldrich, St. Louis, MO, USA). Lysates were centrifuged for 15 min at 12,000 g, and the resulting supernatant was transferred to a new tube and stored at −70 °C. Protein concentrations were determined using a Bradford protein assay kit, and the proteins were separated by electrophoresis and transferred to nitrocellulose membranes. Membranes were blocked for 1.5 h in Tris-buffered saline and Tween 20 (TBST, pH 7.6) containing 5% non-fat dry milk and were then incubated

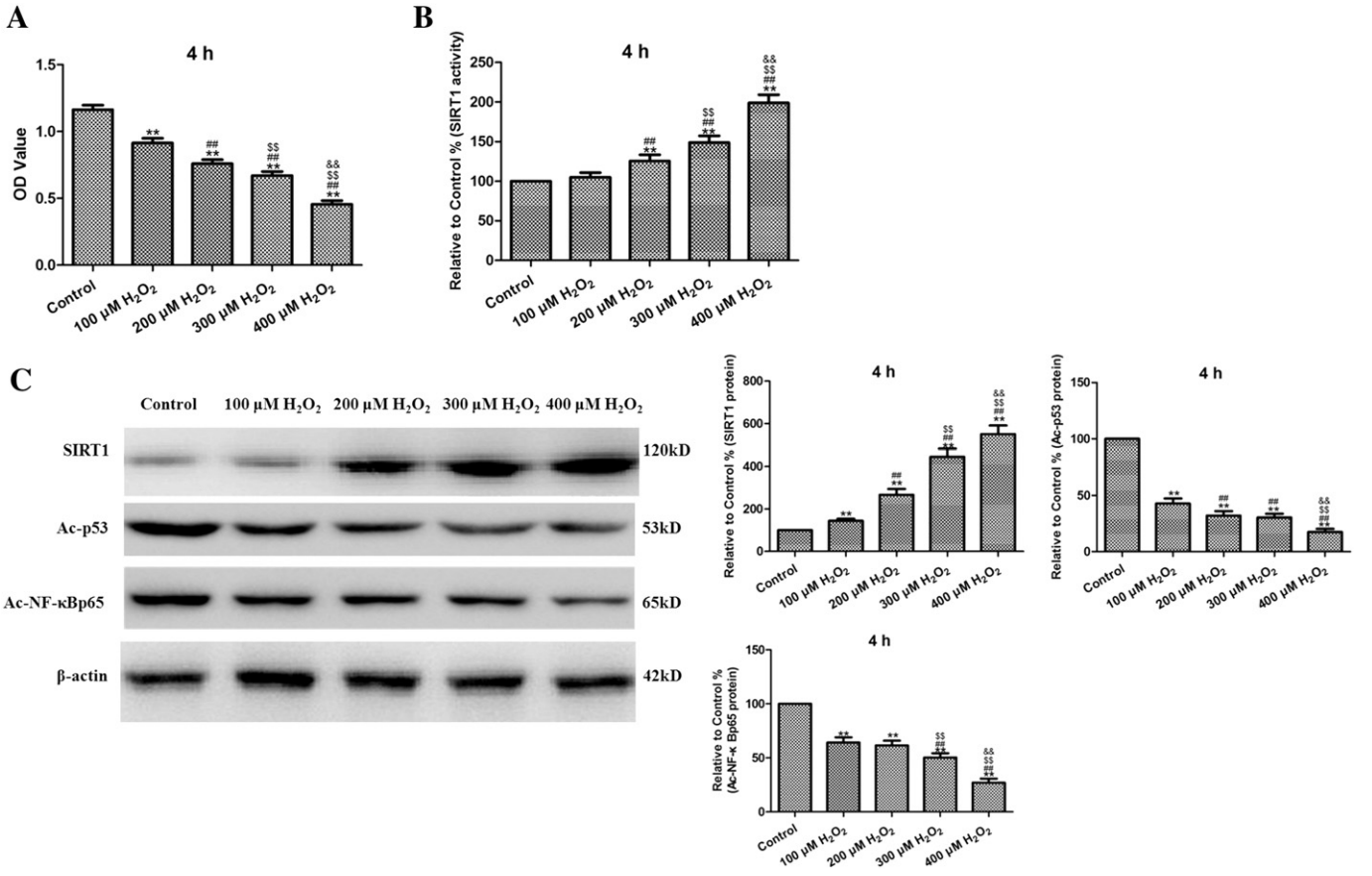

Fig. 1. The effects of H_2O_2 on cell viability, SIRT1 activity, and expression of SIRT1 signaling in HUVECs. A. Cell viability was assessed by performing a CCK8 assay, and the viability was expressed as an OD value. B. SIRT1 activity was detected by ELISA kit. C. Representative Western blots of SIRT1, Ac-p53, and Ac-NF-κBp65 are shown. The results are expressed as the means ± SD, n = 6, $^{**}P < 0.01$ compared with the control group, $^{\#\#}P < 0.01$ compared with the 100 μM H_2O_2 group, $^{\$\$}P < 0.01$ compared with the 200 μM H_2O_2 group, $^{\&\&}P < 0.01$ compared with the 300 μM H_2O_2 group. OD, optical density.

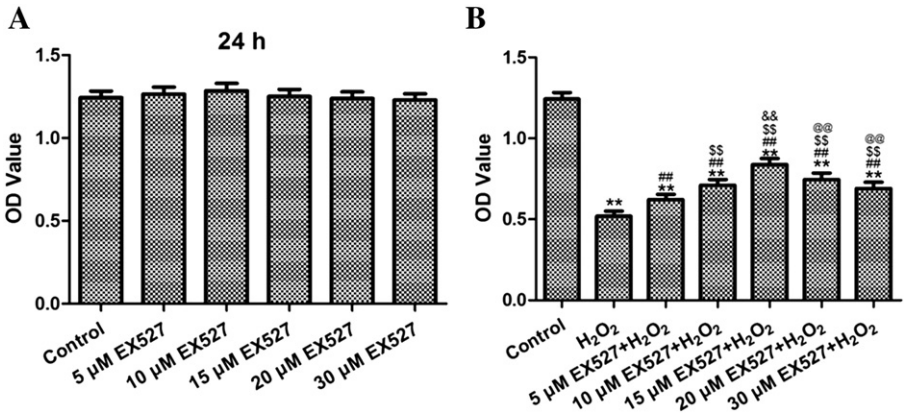

Fig. 2. The effects of EX527 treatment on the viability of normal and H_2O_2-treated HUVECs. A. The effect of EX527 treatment on normal cell viability (24 h). B. The effect of EX527 pretreatment on H_2O_2-treated cell viability. The results are expressed as the means ± SD, n = 6, $^{**}P < 0.01$ compared with the control group, $^{\#\#}P < 0.01$ compared with the H_2O_2 group, $^{\$\$}P < 0.01$ compared with the 5 μM EX527 + H_2O_2 group, $^{\&\&}P < 0.01$ compared with the 10 μM EX527 + H_2O_2 group, $^{@@}P < 0.01$ compared with the 15 μM EX527 + H_2O_2 group. OD, optical density.

overnight at 4 °C with antibodies against SIRT1, p-p38MAPK, p38MAPK, p-JNK, JNK (1:500 dilution), p-ERK, ERK, SOD, GSH-Px, Ac-p53, Ac-NF-κBp65 or β-actin (1:1000 dilution), followed by washes with TBST. The membranes were then probed with the appropriate secondary antibodies (1:5000 dilutions) at room temperature for 90 min and washed with TBST. Protein bands were detected using a Bio-Rad imaging system

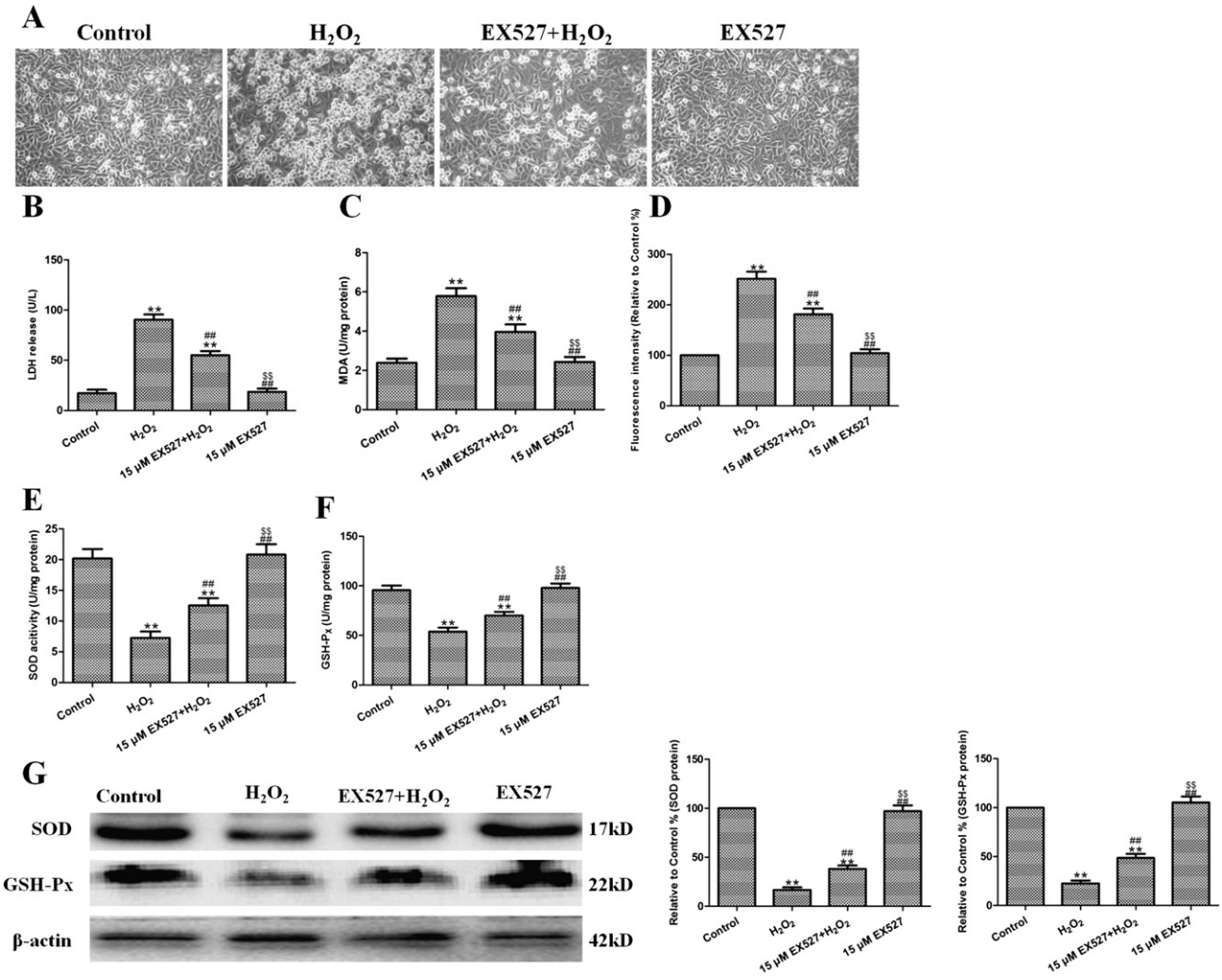

Fig. 3. The effects of EX527 (15 μM) on cell morphology, LDH release, MDA, ROS, SOD, and GSH-Px levels in H_2O_2-injured HUVECs. A. Cell morphology was observed and pictures were taken under an inverted/phase contrast microscope, cell viability was expressed as an OD value. B. LDH release. C. Intracellular MDA levels. D. Intracellular ROS levels. E. Intracellular SOD levels. F. Intracellular GSH-Px levels. G. Representative Western blots of SOD and GSH-Px are shown. The results are expressed as the means ± SD, n = 6, $^{**}P < 0.01$ compared with the control group, $^{\#\#}P < 0.01$ compared with the H_2O_2 group, $^{\$\$}P < 0.01$ compared with the 15 μM EX527 + H_2O_2 group. LDH, lactate dehydrogenase; MDA, methane dicarboxylic aldehyde; ROS, reactive oxygen species; SOD, superoxide dehydrogenase; GSH-Px, glutathione peroxidase.

(Bio-Rad, Hercules, CA, USA) and quantified using the Quantity One software package (West Berkeley, CA, USA).

2.13. Statistical analysis

All values are presented as the mean ± the standard deviation (SD). Group comparisons were performed using an ANOVA (SPSS 13.0). All groups were analyzed simultaneously with an LSD *t* test. A difference of $P < 0.05$ was considered to be statistically significant.

3. Results

3.1. The effects of H_2O_2 on cell viability, SIRT1 activity, and expression of SIRT1 signaling in HUVECs

First, HUVECs were subjected to 4 h H_2O_2 (100, 200, 300, or 400 μM) treatment. The OD value was determined by the CCK8 assay; the decreased OD value indicated reduced cell viability. The OD value in the control group was 1.163 ± 0.034. As expected, incubation with different H_2O_2 concentrations caused a significant decrease in the OD values to 0.914 ± 0.035, 0.759 ± 0.030, 0.671 ± 0.030, 0.456 ± 0.027, respectively ($P < 0.01$ compared with the control group, Fig. 1A). H_2O_2 also increased the SIRT1 activity in a dose-dependent manner ($P < 0.01$ compared with the control group, Fig. 1B). Additionally, H_2O_2 significantly increased SIRT1 protein expression and decreased Ac-p53 and Ac-NF-κBp65 expressions ($P < 0.01$ compared with the control group, Fig. 1C). The effect of 400 μM H_2O_2 was the most apparent, as observed in the increased SIRT1 activity and protein expression of 199.06 ± 10.26% and 550.43 ± 40.65%, respectively, and the decreased Ac-p53 and Ac-NF-κBp65 expressions of 17.51 ± 2.81% and 27.02 ± 3.73%.

3.2. The effects of EX527 on normal and H_2O_2-treated HUVEC viability

Compared with the control group, EX527 treatment (5, 10, 15, 20, or 30 μM) alone for 24 h did not have a significant influence on cell viability (Fig. 2A). To explore the role of the SIRT1 signaling pathway in the H_2O_2-induced OSI in HUVECs, cells were pretreated with EX527 (5, 10, 15, 20, or 30 μM) for 12 h and then subjected to 4 h H_2O_2-induced OSI. The H_2O_2 treatment significantly decreased the OD value to 0.519 ± 0.031 ($P < 0.01$ compared with the control group, Fig. 2B). EX527 treatments significantly increased the OD values to 0.622 ± 0.033, 0.711 ± 0.035, 0.838 ± 0.037, 0.745 ± 0.040, and 0.691 ± 0.038, respectively (all $P < 0.01$ compared with the H_2O_2 group). The protective effect of 15 μM EX527 was the most obvious; thus, this concentration was selected for further study.

3.3. The effects of EX527 on cell morphology, LDH release, MDA, ROS, SOD, and GSH-Px levels in H_2O_2-injured HUVECs

The effects of EX527 on cell morphology, LDH release, intracellular MDA, ROS, SOD, and GSH-Px levels in H_2O_2-injured HUVECs were also explored. As demonstrated in Fig. 3A, H_2O_2 treatment for 4 h resulted

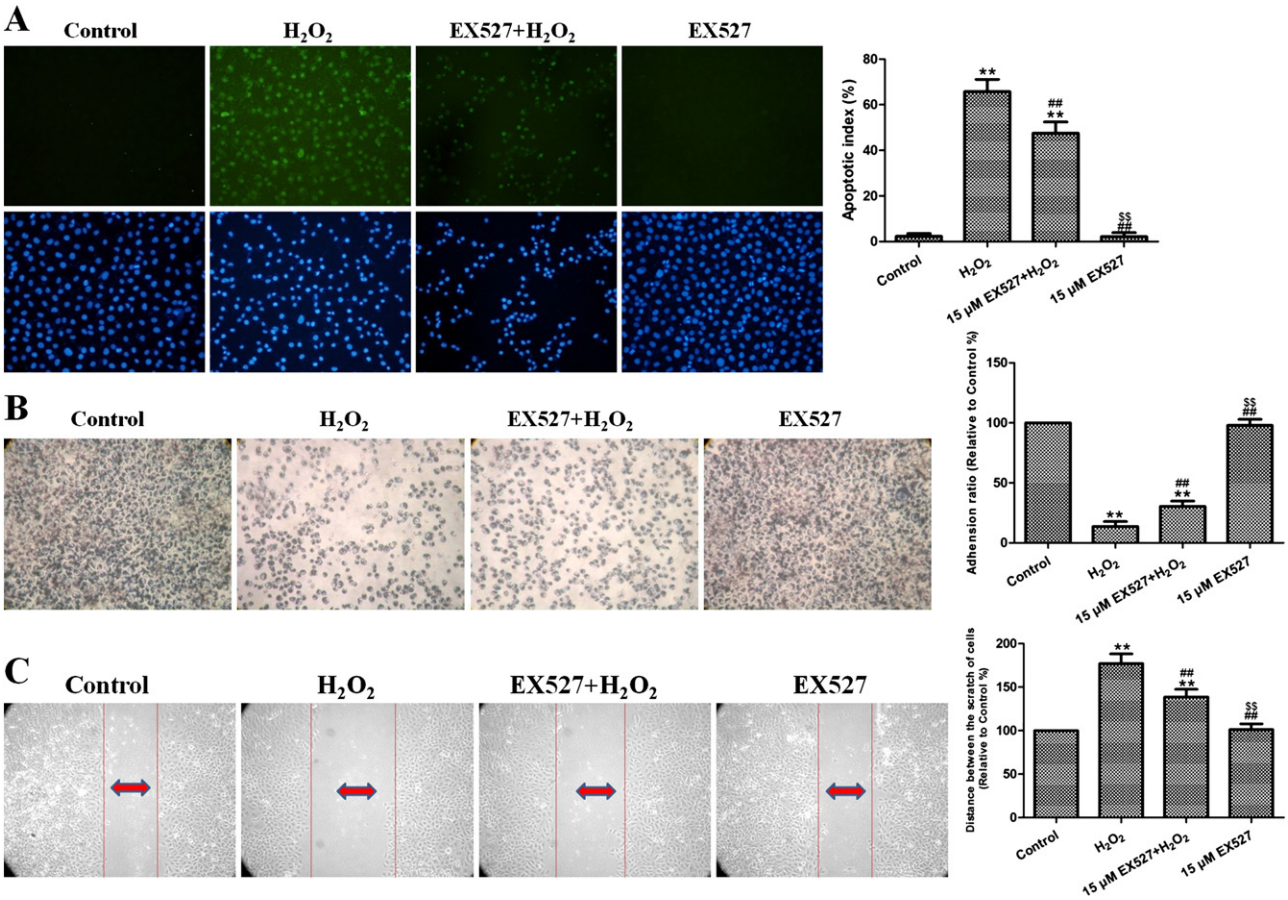

Fig. 4. The effects of EX527 treatment (15 μM) on the cell apoptotic index, adhesive ability, and migratory ability of H_2O_2-injured HUVECs. A. Cellular apoptosis was assessed by performing a TUNEL assay (×200), and apoptosis was expressed as the apoptotic index. TUNEL staining was performed to stain the apoptotic cell nuclei (green), and DAPI was used to stain all nuclei (blue). The apoptotic index was expressed as the ratio of the number of positively stained apoptotic cells to the total number of cells counted × 100%. B. The cell adhesive ability was assessed by performing an adhesion assay (×200), and cell adhesion was expressed as an adhesion ratio. The number of adherent cells in the control group was set to 100%. C. The migratory ability of the cells was assessed by performing a wound healing assay (×100), and migratory ability was expressed as the mean distance between the two ends of the scratch. The mean distance in the control group was set to 100%. The results are expressed as the means ± SD, n = 6, $^{**}P < 0.01$ compared with the control group, $^{\#\#}P < 0.01$ compared with the H_2O_2 group, $^{\$\$}P < 0.01$ compared with the 15 μM EX527 + H_2O_2 group.

in significant cell shrinkage and decreased rates of cellular attachment compared with the control group. Treatment with 15 μM EX527 attenuated H_2O_2-induced cell shrinkage and improved the cellular attachment rate.

H_2O_2 treatment also increased the LDH release and intracellular MDA levels to 94.40 ± 5.18 U/l and 5.78 ± 0.41 U/mg, respectively ($P < 0.01$ compared with control groups, Fig. 3B and C); however, EX527 pretreatment markedly decreased LDH release and intracellular MDA levels to 55.04 ± 4.16 U/l and 3.96 ± 0.38 U/mg, respectively ($P < 0.01$ compared with the H_2O_2 group). Intracellular ROS concentration was determined by measuring the DCFH fluorescence intensity. As demonstrated in Fig. 3D, after H_2O_2 treatment, the fluorescence intensity increased significantly to 251.62 ± 13.97% ($P < 0.01$ compared with the control group). EX527 treatment significantly decreased the fluorescence intensity to 181.24 ± 11.34% ($P < 0.01$ compared with the H_2O_2 group).

Additionally, treating cells with H_2O_2 decreased SOD and GSH-Px levels to 7.25 ± 1.04 U/mg and 53.82 ± 4.16 U/mg, respectively ($P < 0.01$ compared with the control group, Fig. 3E and F). However, EX527 treatment significantly attenuated the changes in SOD and GSH-Px contents to 12.54 ± 1.17 U/mg and 70.10 ± 3.73 U/mg, respectively ($P < 0.01$ compared with the H_2O_2 group). Similar SOD and GSH-Px protein expression results were obtained by Western blot (Fig. 3G). H_2O_2 decreased SOD and GSH-Px expressions to 16.73 ± 2.60% and 22.56 ± 3.04%, respectively ($P < 0.01$ compared with the control group). However, EX527 treatment significantly increased the SOD and GSH-Px expressions to 38.04 ± 3.57% and 48.67 ± 4.11%, respectively ($P < 0.01$ compared with the H_2O_2 group).

3.4. The effects of EX527 treatment on cell apoptotic index, adhesive ability, and migratory ability in H_2O_2-injured HUVECs

After H_2O_2 treatment, the cellular apoptotic index significantly increased to 65.19 ± 5.31% ($P < 0.01$ compared with the control group, Fig. 4A). EX527 treatment significantly decreased the cell apoptotic index to 47.53 ± 4.88% ($P < 0.01$ compared with the H_2O_2 group). H_2O_2 treatment also significantly decreased the cell adhesive ratio to 13.69 ± 4.18%, ($P < 0.01$ compared with the control group, Fig. 4B). EX527 treatment significantly increased the cell adhesive ratio to 30.46 ± 4.37% ($P < 0.01$ compared with the H_2O_2 group). As demonstrated in Fig. 4C, after H_2O_2 treatment, the distance between the scratches increased significantly to 177.14 ± 11.09% ($P < 0.01$ compared with the control group). EX527 treatment significantly decreased the distance to 138.71 ± 8.80% ($P < 0.01$ compared with the H_2O_2 group).

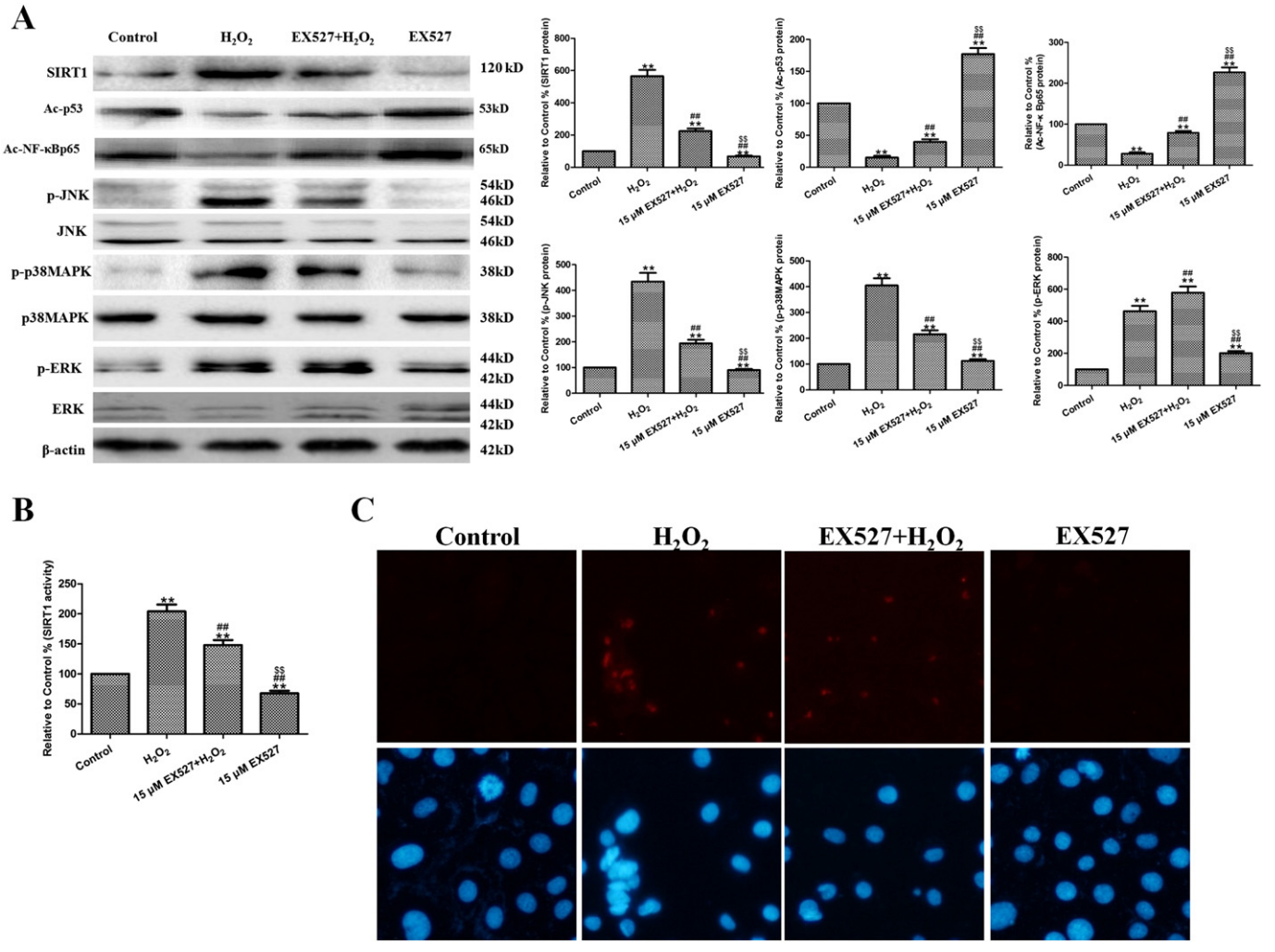

Fig. 5. The effects of EX527 (15 μM) treatment on SIRT activity and SIRT1, p-JNK, p-p38MAPK, and p-ERK protein expressions in H_2O_2-injured HUVECs. A. Representative Western blots of SIRT1, p-JNK, p-p38MAPK, and p-ERK are shown. B. SIRT1 activity was detected by ELISA kit. C. Representative images of SIRT1 immunofluorescence are shown (×200). The results are expressed as the means ± SD, n = 6, $^{**}P < 0.01$ compared with the control group, $^{\#\#}P < 0.01$ compared with the H_2O_2 group, $^{\$\$}P < 0.01$ compared with the 15 μM EX527 + H_2O_2 group. "p-" stands for phosphorylated.

3.5. The effects of EX527 treatment on SIRT1, p-JNK, p-p38MAPK, and p-ERK expressions in H_2O_2-injured HUVECs

Western blot and immunofluorescence results demonstrated that H_2O_2 increased SIRT1 protein expression and activity in HUVECs ($P < 0.01$ compared with the control group, Fig. 5A and B) and that the upregulated SIRT1 was mostly located in the nucleus (Fig. 5C). EX527 pretreatment reversed the H_2O_2 effect on SIRT1 expression and activity ($P < 0.01$ compared with the H_2O_2 group). H_2O_2 treatment also significantly increased p-JNK, p-p38MAPK, and p-ERK expressions compared with the control group ($P < 0.01$), while EX527 treatment reversed these effects on p-JNK and p-p38MAPK but further increased p-ERK expression ($P < 0.01$ compared with the H_2O_2 group).

3.6. The effects of SIRT1 siRNA on cell viability, morphology, LDH release, MDA, ROS, SOD, and GSH-Px levels in H_2O_2-injured HUVECs

To further confirm the role of the SIRT1 signaling pathway in H_2O_2-induced OSI in HUVECs, cells that were pretreated with SIRT1 siRNA for 24 h were subjected to 4 h H_2O_2-induced OSI. SIRT1 siRNA pretreatment significantly reversed the OD value to 0.751 ± 0.034, attenuated H_2O_2-induced cell shrinkage and improved the cellular attachment rate ($P < 0.01$ compared with the control siRNA + H_2O_2 group, Fig. 6A).

As observed in HUVECs treated with EX527, SIRT1 siRNA pretreatment markedly decreased the LDH release and intracellular MDA levels induced by H_2O_2 to 65.42 ± 4.85 U/l and 4.26 ± 0.40 U/mg, respectively ($P < 0.01$ compared with the control siRNA + H_2O_2 group, Fig. 6B and C). EX527 treatment also significantly decreased the ROS level to 215.24 ± 12.06% ($P < 0.01$ compared with the control siRNA + H_2O_2 group).

Additionally, treating cells with H_2O_2 decreased the SOD and GSH-Px levels ($P < 0.01$ compared with the control siRNA group, Fig. 6E and F). SIRT1 siRNA treatment significantly attenuated the changes in SOD and GSH-Px contents to 13.79 ± 1.52 U/mg and 61.20 ± 4.51 U/mg, respectively ($P < 0.01$ compared with the control siRNA + H_2O_2 group). Similar SOD and GSH-Px protein expression results were obtained by Western blot (Fig. 6G). EX527 treatment significantly increased the SOD and GSH-Px expressions to 33.92 ± 3.25% and 34.19 ± 3.48%, respectively ($P < 0.01$ compared with the control siRNA + H_2O_2 group).

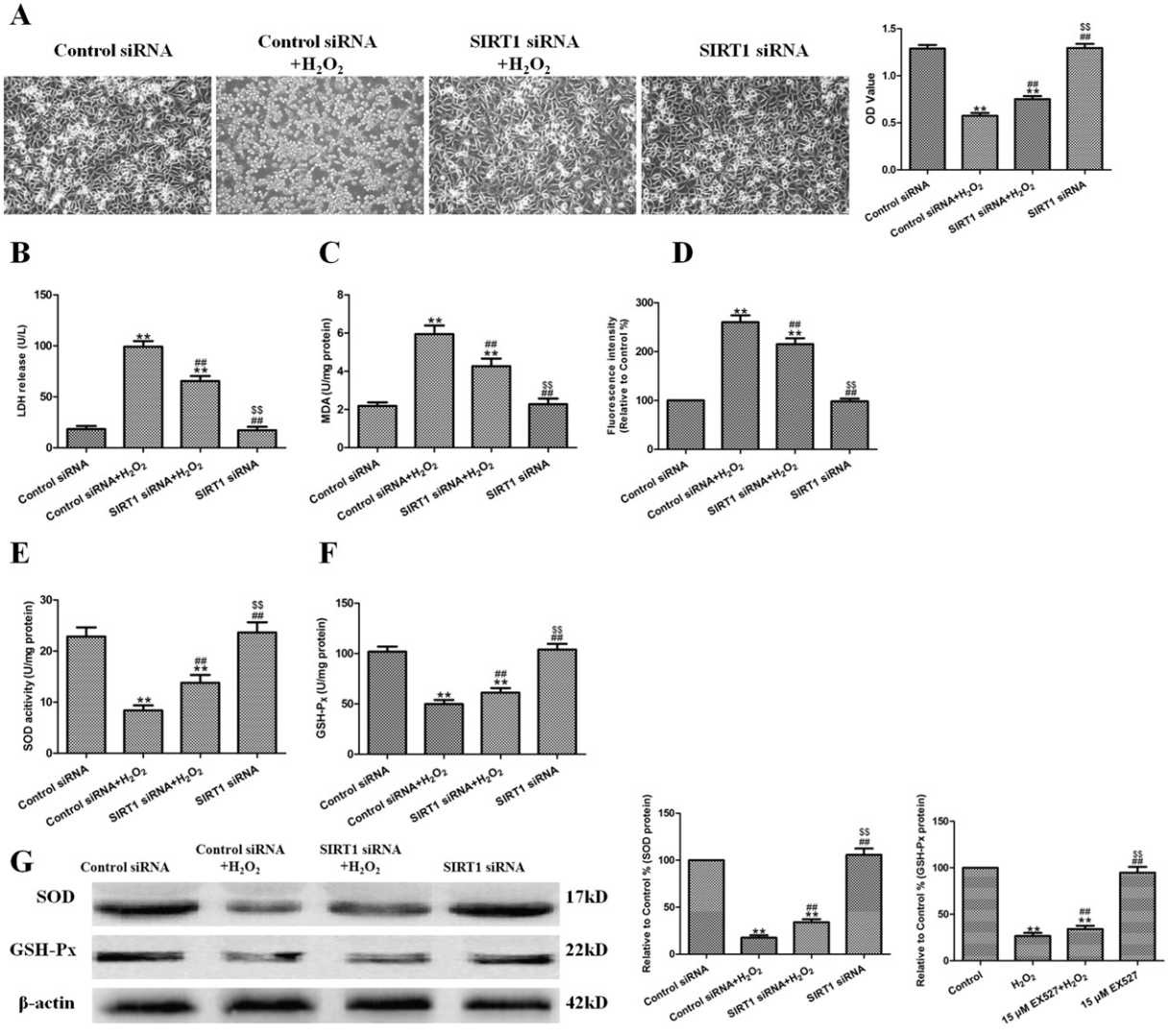

Fig. 6. The effects of SIRT1 siRNA treatment on cell morphology, LDH release, MDA, ROS, SOD, and GSH-Px levels in H_2O_2-injured HUVECs. A. Cell morphology was observed, and pictures were taken under an inverted/phase contrast microscope; cell viability was expressed as an OD value. B. LDH release. C. Intracellular MDA levels. D. Intracellular ROS levels. E. Intracellular SOD levels. F. Intracellular GSH-Px levels. G. Representative Western blots of SOD and GSH-Px are shown. The results are expressed as the means ± SD, n = 6, $^{**}P < 0.01$ compared with the control siRNA group, $^{\#\#}P < 0.01$ compared with the control siRNA + H_2O_2 group, $^{\$\$}P < 0.01$ compared with the SIRT1 siRNA + H_2O_2 group. LDH, lactate dehydrogenase; MDA, methane dicarboxylic aldehyde; ROS, reactive oxygen species; SOD, superoxide dehydrogenase; GSH-Px, glutathione peroxidase.

3.7. The effects of SIRT1 siRNA treatment on cell apoptotic index, adhesive ability, and migratory ability in H_2O_2-injured HUVECs

After H_2O_2 treatment, the cellular apoptotic index increased significantly ($P < 0.01$ compared with the control siRNA group, Fig. 7A). SIRT1 siRNA treatment significantly decreased the cell apoptotic index to 34.74 ± 4.56% ($P < 0.01$ compared with the control siRNA + H_2O_2 group). H_2O_2 treatment also significantly decreased the cell adhesive ratio ($P < 0.01$ compared with the control siRNA group, Fig. 7B). SIRT1 siRNA treatment significantly increased the cell adhesive ratio to 32.61 ± 4.31% ($P < 0.01$ compared with the control siRNA + H_2O_2 group). As demonstrated in Fig. 7C, after H_2O_2 treatment, the distance between scratches significantly increased ($P < 0.01$ compared with the control siRNA group). SIRT1 siRNA treatment significantly decreased the distance to 155.16 ± 8.27% ($P < 0.01$ compared with the control siRNA + H_2O_2 group).

3.8. The effects of SIRT1 siRNA on SIRT1, p-JNK, p-p38MAPK, and p-ERK expressions in H_2O_2-injured HUVECs

Western blot and immunofluorescence results demonstrated that H_2O_2 increased SIRT1 protein expression and activity in HUVECs ($P < 0.01$ compared with the control siRNA group, Fig. 8A and B) and that the upregulated SIRT1 was mostly located in the nucleus (Fig. 8C). SIRT1 siRNA pretreatment reversed the H_2O_2 effect on SIRT1 expression and activity ($P < 0.01$ compared with the control siRNA + H_2O_2 group). H_2O_2 treatment also significantly increased p-JNK, p-p38MAPK, and p-ERK expressions compared with the control siRNA group ($P < 0.01$), while SIRT1 siRNA treatment reversed these effects on p-JNK and p-p38MAPK but further increased p-ERK expression ($P < 0.01$ compared with the control siRNA + H_2O_2 group).

4. Discussion

Recent studies have demonstrated that SIRT1 plays an important role in OSI [11–16]. Many studies have found that SIRT1 is downregulated in OSI and that SIRT1 up-regulation may be beneficial for OSI. For example, Guo and colleagues determined that resveratrol protects HUVECs from oxidized low-density lipoprotein (ox-LDL)-induced oxidative damage via the upregulation of SIRT1 signaling [12]. Hu and colleagues demonstrated that resveratrol attenuated cardiac oxidative damage and left ventricular remodeling and further decreased SIRT1 expression in hearts of old rats with emphysema; thus, decreased SIRT1 levels may be a therapeutic goal for cardiac injury complications in

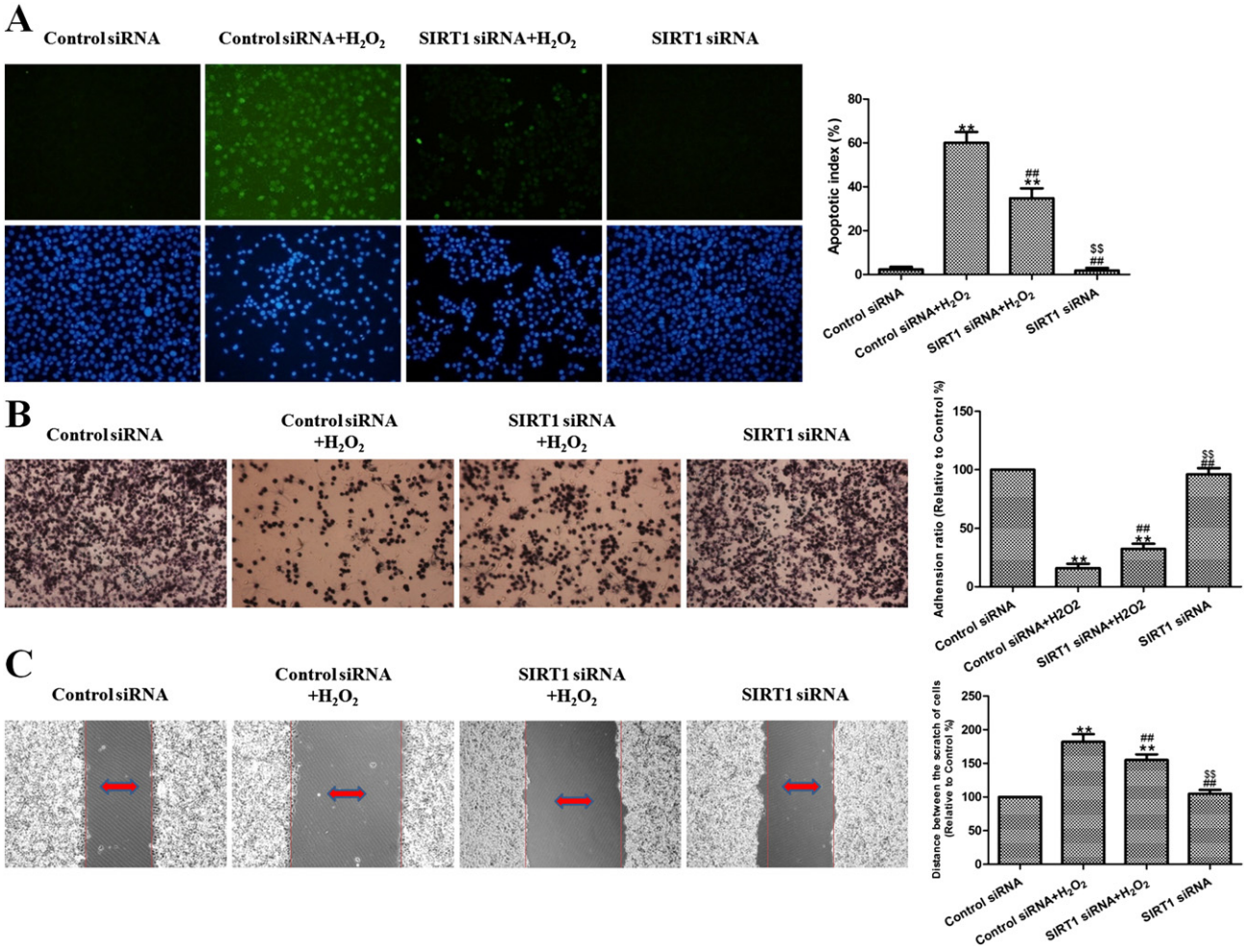

Fig. 7. The effects of SIRT1 siRNA treatment on the cell apoptotic index, adhesive ability, and migratory ability of H_2O_2-injured HUVECs. A. Cellular apoptosis was assessed by performing a TUNEL assay (×200), and apoptosis was expressed as the apoptotic index. TUNEL staining was performed to stain the apoptotic cell nuclei (green), and DAPI was used to stain all nuclei (blue). The apoptotic index was expressed as the ratio of the number of positively stained apoptotic cells to the total number of cells counted × 100%. B. The cell adhesive ability was assessed by performing an adhesion assay (×200), and cell adhesion was expressed as an adhesion ratio. The number of adherent cells in the control group was set to 100%. C. The migratory ability of the cells was assessed by performing a wound healing assay (×100), and migratory ability was expressed as the mean distance between the two ends of the scratch. The mean distance in the control group was set to 100%. The results are expressed as the means ± SD, n = 6, $^{**}P < 0.01$ compared with the control siRNA group, $^{\#\#}P < 0.01$ compared with the control siRNA + H_2O_2 group, $^{\$\$}P < 0.01$ compared with the SIRT1 siRNA + H_2O_2 group.

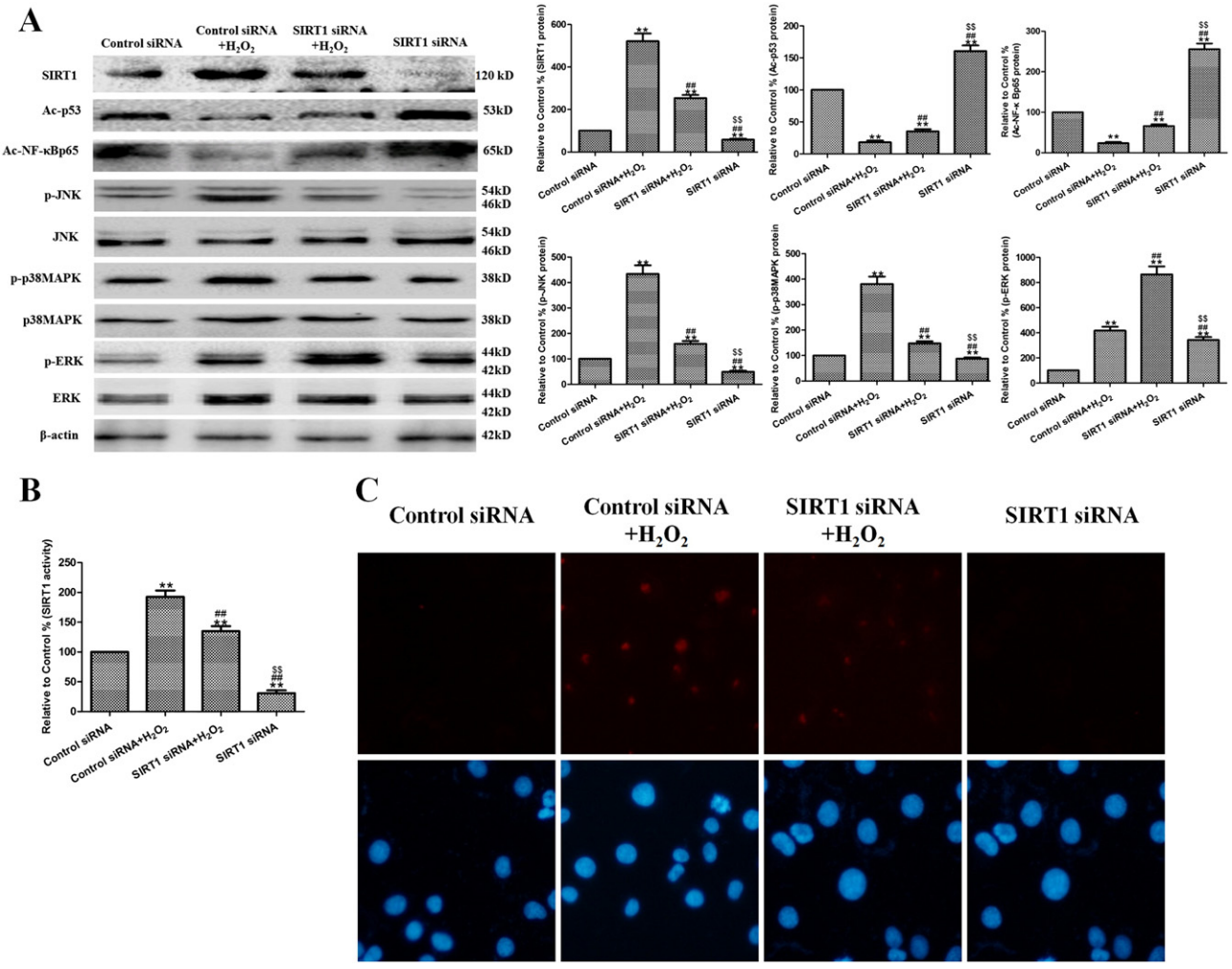

Fig. 8. The effects of SIRT1 siRNA treatment on SIRT activity and SIRT1, p-JNK, p-p38MAPK, and p-ERK protein expressions in H_2O_2-injured HUVECs. A. Representative Western blots of SIRT1, p-JNK, p-p38MAPK, and p-ERK are shown. B. SIRT1 activity was detected using an ELISA kit. Cn Representative images of SIRT1 immunofluorescence are shown (×200). The results are expressed as the means ± SD, n = 6, $^{**}P < 0.01$ compared with the control siRNA group, $^{\#\#}P < 0.01$ compared with the control siRNA + H_2O_2 group, $^{\$\$}P < 0.01$ compared with the SIRT1 siRNA + H_2O_2 group.

chronic obstructive pulmonary disease (COPD) [13]. However, other studies have demonstrated that SIRT1 is up-regulated in OSI. For example, Lim and colleagues determined that H_2O_2 treatment significantly increased SIRT1 expression in human chondrocytes, and the incubation of these cells with melatonin decreased H_2O_2-induced SIRT1 mRNA and protein expressions [15]. Brandl and colleagues also demonstrated that SIRT1 was up-regulated after sub-lethal doses of oxidative stress (induced by H_2O_2), and its expression levels increased in aging mesenchymal stem cells [16]. Furthermore, a few studies noted that SIRT1 activation is not always beneficial for fighting diseases [9,10]. Therefore, it is unclear whether SIRT1 is inhibited or activated by OSI. The varying effects may depend on the duration of injury time, the type of injury-inducing drugs or methods, and when injury interventions are initiated. Interestingly, we determined that chronic and mild oxidative stress stimulations (e.g., ox-LDL, COPD, and cigarette smoke extract) mostly downregulated SIRT1, while acute and serious stimulations (H_2O_2) mostly upregulated SIRT1. In this study, we determined that acute OSI induced by H_2O_2 significantly injured the HUVECs and increased SIRT1 protein expression. EX527, a specific SIRT1 inhibitor, conferred a protective effect on the HUVECs against H_2O_2, as indicated by the improved cell viability, adhesive ability, migratory ability, and decreased apoptotic index. EX527 also effectively inhibited H_2O_2-induced SIRT1 upregulation. Studies have shown that EX527 also affects SIRT2 activity in the low concentration range [26], so it is unclear if some of the effects of EX527 are not due to inhibition of SIRT2. Therefore, further SIRT1 siRNA experiments were carried out to verify the role of SIRT1 in acute endothelial OSI. Similar results were confirmed in SIRT1 siRNA experiments. These results demonstrate that SIRT1 signaling pathway inhibition protects against acute OSI in endothelial cells.

During the process of OSI-induced apoptosis or death, mitochondria serve as a source of ROS, which is generated by reducing the mitochondrial membrane potential; the enhanced ROS production is related to the OSI-induced injury response [5,27]. Lipid peroxidation is one of the primary events in cell OSI [28]. MDA is a by-product of the lipid peroxidation induced by excessive ROS that is widely used as a biomarker of oxidative stress. However, cells are equipped with several antioxidants, such as SOD and GSH-Px, along with other enzymatic and non-enzymatic antioxidants for the prevention of free-radical damage and ROS-induced cellular damage [3]. Therefore, intracellular ROS can be effectively eliminated by the combined action of SOD, GSH-Px and other endogenous antioxidants and thus provide a repair mechanism for oxidized membrane components [3,28]. In the present study, significant decreases in SOD and GSH-Px were observed in HUVECs after H_2O_2 exposure, indicating an impairment in antioxidant defenses. A significant increase in MDA production was associated with increased LDH release. Nonetheless, when HUVECs were pretreated with EX527, these H_2O_2-

induced cellular events were blocked. Similar results were confirmed in the SIRT1 siRNA experiments. These results suggest that the enhancement of endogenous antioxidant preservation may represent a major cellular protective mechanism by inhibiting SIRT1 signaling.

MAPKs are a family of serine/threonine kinases and are important signaling components that link extracellular stimuli to a multitude of intracellular responses that affect cell growth, differentiation, survival, and metabolic regulation [17,18,29]. There are 3 major MAPK classes that have been described: ERK1/2, of which two major isoforms, p44 (ERK-1) and p42 (ERK-2), have been identified; p38MAPK; and JNK [29]. JNK is also known as a stress-activated protein kinase, and p38MAPK is primarily involved in cell responses to cytotoxic agents and stress [29,30]. Studies also have demonstrated that JNK, p38MAPK, and ERK are involved in endothelial cell OSI [17,18], which are phosphorylated early in the response to OSI [19]. Transient activation of these kinases in response to OSI cytokines promotes endothelial cell proliferation and survival, while prolonged activation of these kinases may result in endothelial cell death through modulation of pro- and anti-apoptotic protein functions [20,21]. SIRT1 may also cross-talk with the MAPKs to regulate various physiological and pathological processes [15,31]. In the simulated cardiomyocyte ischemia reperfusion model, Becatti and colleagues demonstrated that SIRT1 overexpression positively affected the p38MAPK pathway via protein kinase B(Akt)/apoptosis signal-regulating kinase 1 (ASK1) signaling by reducing p38 and JNK phosphorylation and increasing ERK phosphorylation [32]. Another study found that melatonin exerted cytoprotective and anti-inflammatory effects in an oxidative stress-stimulated chondrocyte model and rabbit osteoarthritis model and that the SIRT1 pathway was strongly involved in this effect. In this procedure, melatonin blocked H O -induced phosphorylation of PI3K/Akt, p38, ERK, JNK, and MAPK, as well as the activation of NF-κB, which was reversed by SIRT1 inhibitor or SIRT1 siRNA [12]. Thus, we also explored the effects of SIRT1 on these MAPKs in endothelial cell OSI. Western blotting demonstrated that H_2O_2 treatment increased p-JNK, p-p38MAPK, and p-ERK expressions. Treatment with EX527 reversed these effects on p-JNK and p-p38MAPK, but further increased p-ERK expression. Similar results were confirmed in SIRT1 siRNA experiments. Thus, ERK signaling may be contributed to the anti-OSI effect of SIRT1 inhibition.

In summary, our study demonstrates that inhibiting SIRT1 signaling confers protection against acute endothelial OSI and that the SIRT1 signaling pathway is a crucial mediator of endothelial OSI, modulation of MAPKs (JNK, p38MAPK, and ERK) may be involved in the protective effect of SIRT1 inhibition.

Conflict of interest

No potential conflict of interest relevant to this article was disclosed.

Acknowledgements

This study was supported by grants from the Excellent Doctoral Support Project of the Fourth Military Medical University (2013D01), the National Natural Science Foundation of China (81070951, 81222015, 81000938, 81170213, 81102091), the New Century Talent Supporting Project by Chinese Education Ministry (NCET-12-1004), and the Chinese Changjiang Scholars and Innovative Research Team in University (IRT1053).

References

[1] N. Valtcheva, A. Primorac, G. Jurisic, M. Hollmén, M. Detmar, The orphan adhesion G protein-coupled receptor GPR97 regulates migration of lymphatic endothelial cells via the small GTPases RhoA and Cdc42, J. Biol. Chem. 288 (2013) 35736–35748.
[2] C.A. Chen, T.Y. Wang, S. Varadharaj, L.A. Reyes, C. Hemann, M.A. Talukder, Y.R. Chen, L.J. Druhan, J.L. Zweier, S-glutathionylation uncouples eNOS and regulates its cellular and vascular function, Nature 468 (2010) 1115–1118.
[3] Y. Yang, W. Duan, Z. Liang, W. Yi, J. Yan, N. Wang, Y. Li, W. Chen, S. Yu, Z. Jin, D. Yi, Curcumin attenuates endothelial cell oxidative stress injury through Notch signaling inhibition, Cell. Signal. 25 (2013) 615–629.
[4] L. Polidoro, G. Properzi, F. Marampon, G.L. Gravina, C. Festuccia, E. Di Cesare, L. Scarsella, C. Ciccarelli, B.M. Zani, C. Ferri, Vitamin D protects human endothelial cells from H O oxidant injury through the Mek/Erk-Sirt1 axis activation, J. Cardiovasc. Transl. Res. 6 (2013) 221–231.
[5] W. Duan, Y. Yang, W. Yi, J. Yan, Z. Liang, N. Wang, Y. Li, W. Chen, S. Yu, Z. Jin, D. Yi, New role of JAK2/STAT3 signaling in endothelial cell oxidative stress injury and protective effect of melatonin, PLoS One 8 (2013) e57941.
[6] V. Mugoni, R. Postel, V. Catanzaro, E. De Luca, E. Turco, G. Digilio, L. Silengo, M.P. Murphy, C. Medana, D.Y. Stainier, J. Bakkers, M.M. Santoro, Ubiad1 is an antioxidant enzyme that regulates eNOS activity by CoQ10 synthesis, Cell 152 (2013) 504–518.
[7] Y. Yang, W. Duan, Y. Li, Z. Jin, J. Yan, S. Yu, D. Yi, Novel role of silent information regulator 1 in myocardial ischemia, Circulation 128 (2013) 2232–2240.
[8] Y. Yang, W. Duan, Y. L, J. Yan, W. Yi, Z. Liang, N. Wang, D. Yi, Z. Jin, New role of silent information regulator 1 in cerebral ischemia. Neurobiol, Aging 34 (2013) 2879–2888.
[9] T. Kawashima, Y. Inuzuka, J. Okuda, T. Kato, S. Niizuma, Y. Tamaki, Y. Iwanaga, A. Kawamoto, M. Narazaki, T. Matsuda, S. Adachi, G. Takemura, T. Kita, T. Kimura, T. Shioi, Constitutive SIRT1 overexpression impairs mitochondria and reduces cardiac function in mice, J. Mol. Cell. Cardiol. 51 (2011) 1026–1036.
[10] Y. Li, W. Xu, M.W. McBurney, V.D. Longo, SirT1 inhibition reduces IGF-I/IRS-2/Ras/ERK1/2 signaling and protects neurons, Cell Metab. 8 (2008) 38–48.
[11] J.W. Hwang, I.K. Sundar, H. Yao, M.T. Sellix, I. Rahman, Circadian clock function is disrupted by environmental tobacco/cigarette smoke, leading to lung inflammation and injury via a SIRT1–BMAL1 pathway, FASEB J. 28 (2014) 176–194.
[12] H. Guo, Y. Chen, L. Liao, W. Wu, Resveratrol protects HUVECs from oxidized-LDL induced oxidative damage by autophagy upregulation via the AMPK/SIRT1 pathway, Cardiovasc. Drugs Ther. 27 (2013) 189–198.
[13] Y.X. Hu, H. Cui, L. Fan, X.J. Pan, J.H. Wu, S.Z. Shi, S.Y. Cui, Z.M. Wei, L. Liu, Resveratrol attenuates left ventricular remodeling in old rats with COPD induced by cigarette smoke exposure and LPS instillation, Can. J. Physiol. Pharmacol. 91 (2013) 1044–1054.
[14] Y. Yang, W. Duan, Y. Lin, W. Yi, Z. Liang, J. Yan, N. Wang, C. Deng, S. Zhang, Y. Li, W. Chen, S. Yu, D. Yi, Z. Jin, SIRT1 activation by curcumin pretreatment attenuates mitochondrial oxidative damage induced by myocardial ischemia reperfusion injury, Free Radic. Biol. Med. 65C (2013) 667–679.
[15] H.D. Lim, Y.S. Kim, S.H. Ko, I.J. Yoon, S.G. Cho, Y.H. Chun, B.J. Choi, E.C. Kim, Cytoprotective and anti-inflammatory effects of melatonin in hydrogen peroxide-stimulated CHON-001 human chondrocyte cell line and rabbit model of osteoarthritis via the SIRT1 pathway, J. Pineal Res. 53 (2012) 225–237.
[16] A. Brandl, M. Meyer, V. Bechmann, M. Nerlich, P. Angele, Oxidative stress induces senescence in human mesenchymal stem cells, Exp. Cell Res. 317 (2011) 1541–1547.
[17] S.G. Han, B. Newsome, B. Hennig, Titanium dioxide nanoparticles increase inflammatory responses in vascular endothelial cells, Toxicology 306 (2013) 1–8.
[18] T.C. Hung, L.W. Huang, S.J. Su, B.S. Hsieh, H.L. Cheng, Y.C. Hu, Y.H. Chen, C.C. Hwang, K.L. Chang, Hemeoxygenase-1 expression in response to arecoline-induced oxidative stress in human umbilical vein endothelial cells, Int. J. Cardiol. 151 (2011) 187–194.
[19] H. Yamawaki, K. Saito, M. Okada, Y. Hara, Methylglyoxal mediates vascular inflammation via JNK and p38 in human endothelial cells, Am. J. Physiol. Cell Physiol. 295 (2008) C1510–1517.
[20] C. Mazière, C. Gomila, J.C. Mazière, Oxidized low-density lipoprotein increases osteopontin expression by generation of oxidative stress, Free Radic. Biol. Med. 48 (2010) 1382–1387.
[21] C.L. Hsu, Y.L. Wu, G.J. Tang, T.S. Lee, Y.R. Kou, Ginkgo biloba extract confers protection from cigarette smoke extract-induced apoptosis in human lungendothelial cells: Role of heme oxygenase-1, Pulm. Pharmacol. Ther. 22 (2009) 286–296.
[22] M. Koizumi, J. Tatebe, I. Watanabe, J. Yamazaki, T. Ikeda, T. Morita, Aryl hydrocarbon receptor mediates indoxyl sulfate-induced cellular senescence in human umbilical vein endothelial cells, J. Atheroscler. Thromb. (2014) (Epub ahead of print).
[23] L. Hummitzsch, K. Zitta, B. Bein, M. Steinfath, M. Albrecht, Culture media from hypoxia conditioned endothelial cells protect human intestinal cells from hypoxia/reoxygenation injury, Exp. Cell Res. 322 (2014) 62–70.
[24] X. Gong, Y. Ma, Y. Ruan, G. Fu, S. Wu, Long-term atorvastatin improves age-related endothelial dysfunction by ameliorating oxidative stress and normalizing eNOS/iNOS imbalance in rat aorta, Exp. Gerontol. 52 (2014) 9–17.
[25] S.Z. Safi, R. Qvist, G.O. Yan, I.S. Ismail, Differential expression and role of hyperglycemia induced oxidative stress in epigenetic regulation of β1, β2 and β3-adrenergic receptors in retinal endothelial cells, BMC Med. Genomics 7 (2014) 29.
[26] X. Zhao, D. Allison, B. Condon, F. Zhang, T. Gheyi, A. Zhang, S. Ashok, M. Russell, I. MacEwan, Y. Qian, J.A. Jamison, J.G. Luz, The 2.5 Å crystal structure of the SIRT1 catalytic domain bound to nicotinamide adenine dinucleotide (NAD+) and an indole (EX527 analogue) reveals a novel mechanism of histone deacetylase inhibition, J. Med. Chem. 14 (2013) 963–969.
[27] Z. Liu, D. Li, W. Zhao, X. Zheng, J. Wang, E. Wang, A potent lead induces apoptosis in pancreatic cancer cells, PLoS One 7 (2012) e37841.
[28] H.T. Liu, W.M. Li, G. Xu, X.Y. Li, X.F. Bai, P. Wei, C. Yu, Y.G. Du, Chitosan oligosaccharides attenuate hydrogen peroxide-induced stress injury in human umbilical vein endothelial cells, Pharmacol. Res. 59 (2009) 167–175.

[29] L.H. Osaki, P. Gama, MAPKs and signal transduction in the control of gastrointestinal epithelial cell proliferation and differentiation, Int. J. Mol. Sci. 14 (2013) 10143–10161.
[30] W. Peti, R. Page, Molecular basis of MAP kinase regulation, Protein Sci. 22 (2013) 1698–1710.
[31] G.J. Park, Y.S. Kim, K.L. Kang, S.J. Bae, H.S. Baek, Q.S. Auh, Y.H. Chun, B.H. Park, E.C. Kim, Effects of sirtuin 1 activation on nicotine and lipopolysaccharide-induced cytotoxicity and inflammatory cytokine production in human gingival fibroblasts, J. Periodontal Res. 48 (2013) 483–492.
[32] M. Becatti, N. Taddei, C. Cecchi, N. Nassi, P.A. Nassi, C. Fiorillo, SIRT1 modulates MAPK pathways in ischemic-reperfused cardiomyocytes, Cell. Mol. Life Sci. 69 (2012) 2245–2260.